PHYSICAL REVIEW B **82**, 100414(R) (2010)

Incompatible magnetic order in multiferroic hexagonal $DyMnO_3$

C. Wehrenfennig,[1] D. Meier,[1] Th. Lottermoser,[1] Th. Lonkai,[2] J.-U. Hoffmann,[3] N. Aliouane,[3] D. N. Argyriou,[3] and M. Fiebig[1,*]

[1]*HISKP, Universität Bonn, Nussallee 14-16, 53115 Bonn, Germany*

[2]*Ganerben-Gymnasium, Mühlbergstraße 65, 74653 Künzelsau, Germany*

[3]*Helmholtz-Zentrum Berlin für Materialien und Energie, Hahn Meitner Platz 1, 14109 Berlin, Germany*

(Received 6 September 2010; published 27 September 2010)

Magnetic order of the manganese and rare-earth lattices according to different symmetry representations is observed in multiferroic hexagonal (h-) $DyMnO_3$ by optical second-harmonic generation and neutron diffraction. The incompatibility reveals that the $3d$-$4f$ coupling in the h-RMnO$_3$ system (R=Sc, Y, In, Dy–Lu) is less rigid than commonly expected. Instead, a triggered magnetic phase transition is introduced that constitutes a framework for magnetic and magnetoelectric coupling effects in the h-RMnO$_3$ system.

DOI: 10.1103/PhysRevB.82.100414 PACS number(s): 75.85.+t, 75.25.−j, 75.30.Et, 42.65.Ky

Controlling magnetism by electric fields and (di)electric properties by magnetic fields poses a great challenge to contemporary condensed-matter physics. Possibly the most fertile source for such "magnetoelectric" cross correlations are compounds with a coexistence of magnetic and electric long-range order, called multiferroics.[1] Aside from the magnetically induced ferroelectrics[2] and the ambient multiferroic $BiFeO_3$ (Ref. 3) a system at the center of intense discussion is hexagonal (h-) RMnO$_3$ with R=Sc, Y, In, Dy–Lu.[4] The system displays a variety of multiferroic phases and a "giant" magnetoelectric effect.[5] The availibility of as many as nine h-RMnO$_3$ compounds is ideal for investigating the role of $3d$-$4f$ interactions in the manifestation of magnetoelectric effects, a key question of multiferroics research.

Thus far, it is assumed that the $3d$-$4f$ interaction in the h-RMnO$_3$ leads to a rigid correlation between the magnetic Mn^{3+} and R^{3+} order.[6–11] The Mn^{3+}-R^{3+} exchange paths are affected by the ferroelectric distortion of the unit cell so that it is expected that, reminiscent of the orthorhombic manganites,[2] the $3d$-$4f$ interaction plays a substantial role in the magnetoelectric behavior, including giant magnetoelectric[5] and magnetoelastic[12,13] effects.

In this Rapid Communication we show that the $3d$-$4f$ coupling in h-RMnO$_3$ is substantially less rigid than assumed up to now. This is concluded from optical second harmonic generation (SHG) and supplementary neutron-diffraction data. They reveal that the Mn^{3+} spins and the Dy^{3+} spins in h-$DyMnO_3$ order according to different symmetry representations unless magnetization fields are present. Based on this observation, a triggering mechanism with biquadratic coupling of the R^{3+} and Mn^{3+} magnetic moments is proposed that constitutes a general framework for describing the magnetic structure and the magnetoelectric interactions in the multiferroic h-RMnO$_3$ system.

The h-RMnO$_3$ compounds display ferroelectric ordering at T_C=650–990 K, antiferromagnetic Mn^{3+} ordering at T_N=66–130 K,[4] and, for R=Dy–Yb, magnetic R^{3+} ordering and reordering at T_N and 4–8 K, respectively.[4,6,8,9,14] The spontaneous polarization is 5.6 $\mu C/cm^2$ and directed along z. Frustration leads to a variety of triangular antiferromagnetic structures of the Mn^{3+} spins in the basal xy plane. In contrast, the R^{3+} sublattices order Ising-type along the hexagonal z axis. The possible magnetic structures of the Mn^{3+} and R^{3+} lattices correspond to four one-dimensional representations, see Table I. As we will see, they consistently explain our data so that other representations denoting more complex symmetries[6,14,16] are not listed. An extensive investigation of the magnetic R^{3+} order commenced not long ago and revealed that in h-$HoMnO_3$ and h-$YbMnO_3$ the Mn^{3+} and the R^{3+} order obeys the same representation.[6,8,17]

The compound with the largest R^{3+} ion in the h-RMnO$_3$ series is h-$DyMnO_3$ which was recently grown.[18] The magnetic structure of the Dy^{3+} lattice was investigated by resonant x-ray diffraction and magnetization measurements.[14,18] In an extended analysis its magnetic point group was shown to be $P6_3cm$ in the interval 10 K$<T<T_N$ ("high-temperature range"). At $T<10$ K ("low-temperature range") or above a critical magnetic field applied along z it changes to $P6_3cm$. In this work we focus on the determination of the complementary Mn^{3+} order by SHG but we also corroborate the consistency of the proposed Mn^{3+} and Dy^{3+} order by prominent magnetic neutron-diffraction reflections.

SHG is described by the equation $P_i(2\omega)=\varepsilon_0\chi_{ijk}E_j(\omega)E_k(\omega)$. An electromagnetic light field $\vec{E}$ at frequency ω is incident on a crystal, inducing a dipole oscillation $\vec{P}(2\omega)$, which acts as source of a frequency-doubled light wave of the intensity $I_{SHG}\propto|\vec{P}(2\omega)|^2$. The susceptibility χ_{ijk} couples incident light fields with polarizations j and k to a SHG contribution with polarization i. The magnetic and crystallographic symmetry of a compound is uniquely related to the set of nonzero components χ_{ijk}.[15,19]

The h-$DyMnO_3$ single crystals were obtained by the floating zone technique. SHG reflection spectroscopy with 120 fs laser pulses was conducted on polished z-oriented samples in a ^{4}He-operated cryostat generating magnetic fields of up to 8 T.[19] Neutron diffraction in the $(h0l)$ plane was conducted at the E2 beamline of the Helmholtz-Zentrum at 2.39 Å with the sample mounted in a ^{3}He/^{4}He dilution insert. The crystallographic reflexes for $2\theta=10°-86°$ were observed so that extinction by Dy absorption can be excluded.

In Table I the configurations identifying the magnetic structure of the Mn^{3+} and Dy^{3+} lattices are listed. SHG is only sensitive to the Mn^{3+} order with χ_{xxx} and χ_{yyy} as independent tensor components.[15] Neutron diffraction can probe the magnetic moments of Mn^{3+} and Dy^{3+}. The observation of

TABLE I. Configurations for SHG and neutron diffraction distinguishing between the four major one-dimensional symmetry representations of the crystallographic space group $P6_3cm$ of h-RMnO$_3$. Symmetries refer to the magnetic structure of the Mn^{3+} or Dy^{3+} *subsystem*; the overall symmetry is determined by the intersection of the respective symmetries. Sketches of the magnetic structures of the Mn^{3+} and Dy^{3+} sublattices are given in Refs. 5 and 14. SHG selection rules were derived from Ref. 15. The contributions by the Mn^{3+} and Dy^{3+} lattices to neutron diffraction were calculated *separately* by setting $[\vec{\mu}_{Mn^{3+}} \neq 0,\ \vec{\mu}_{Dy^{3+}}=0]$ and $[\vec{\mu}_{Mn^{3+}}=0,\ \vec{\mu}_{Dy^{3+}} \neq 0]$, respectively, for the magnetic moments. The total yield follows from the interference of the Mn^{3+} and Dy^{3+} contributions (not needed here). The largest value obtained for each sublattice corresponds to 100%.

Representation Symmetry		Γ_1, A_1 $P6_3cm$	Γ_2, A_2 $P6_3\underline{cm}$	Γ_3, B_1 $P\underline{6_3}cm$	Γ_4, B_2 $P\underline{6_3}\underline{cm}$
SHG (Mn^{3+})	χ_{xxx}	0	0	0	$\neq 0$
	χ_{yyy}	0	0	$\neq 0$	0
Neutron (Mn^{3+})	(100)	58%	0	62%	0
	(101)	17%	100%	17%	93%
Neutron (Dy^{3+})	(100)	0	100%	0	75%
	(101)	100%	0	2%	0

the (100) and (101) reflections already leads to very clear results so that we restrict the discussion to them. The contributions by Mn^{3+} and Dy^{3+} moments were separated by assuming $[\vec{\mu}_{Mn^{3+}} \neq 0,\ \vec{\mu}_{Dy^{3+}}=0]$ and $[\vec{\mu}_{Mn^{3+}}=0,\ \vec{\mu}_{Dy^{3+}} \neq 0]$, respectively, for the magnetic moments in the computations done with SIMREF 2.6.[8]

We first focus on the high-temperature range and measurements at zero magnetic field. Figure 1 shows the analysis of the magnetic structure of the Mn^{3+} lattice by SHG spectroscopy. Because of the large optical absorption the SHG data on h-DyMnO$_3$ cannot be taken with the standard transmission setup and nanosecond laser pulses[19]—in contrast to

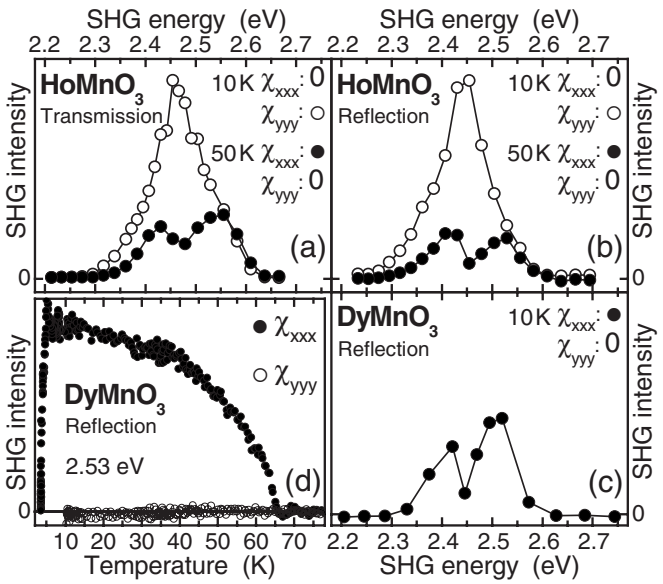

FIG. 1. Spectral, polarization, and temperature dependence of SHG in h-RMnO$_3$ compounds. A "0" indicates zero SHG intensity. [(a) and (b)] SHG spectra of h-HoMnO$_3$ measured in (a) transmission and (b) reflection with a femtosecond laser. (c) SHG spectra of h-DyMnO$_3$ measured in reflection with a femtosecond laser. (d) Temperature dependence of the signal in (c).

all other h-RMnO$_3$ compounds. Instead the reflected SHG signal was measured with a femtosecond laser system. With femtosecond laser pulses, higher-order SHG contributions, incoherent multiphoton processes, and ultrafast nonequilibrium effects can easily obscure any magnetically induced SHG.[19,20] In the first step we therefore had to verify to what extent SHG is still a feasible probe for the magnetic structure. We chose h-HoMnO$_3$ for this test since it allows us to compare transmission and reflection data. Figure 1(a) shows the SHG transmission spectrum taken at two different temperatures with a femtosecond laser system. Aside from a minor decrease in resolution the femtosecond laser pulses lead to the same SHG spectra as the nanosecond laser pulses.[19] With SHG from χ_{xxx} at 50 K and from χ_{yyy} at 10 K we identify the $P6_3cm$ and the $P6_3\underline{cm}$ structures, respectively, on the basis of Table I. Note that the spectral dependence is also characteristic for the respective phases.[21] Figure 1(b) shows the corresponding SHG reflection spectra. Aside from a 98% decrease in the SHG yield the result remains unchanged. Hence, the femtosecond reflection data are well suited for identifying the magnetic phase of h-RMnO$_3$ by SHG. Figures 1(c) and 1(d) show the spectral and temperature dependence of the SHG signal in h-DyMnO$_3$ in a femtosecond reflection experiment. Comparison with Fig. 1(b) and Table I clearly reveals $P6_3\underline{cm}$ as magnetic symmetry of the Mn^{3+} lattice in the high-temperature range up to T_N=66 K. This is an utterly surprising result because $P6_3\underline{cm}$ does not match the $P\underline{6_3}\underline{cm}$ symmetry of the Dy^{3+} lattice proposed in Ref. 14. We therefore sought supplementary confirmation by neutron diffraction.

In Fig. 2 we show the temperature dependence of the (101) and (100) reflections of h-DyMnO$_3$. Note that while the (101) reflection is magnetic in origin, the (100) reflection in the high-temperature range is expected to be purely structural in nature with no magnetic contributions. For the set of symmetries discussed in Table I, zero (100) intensity is only possible if the magnetic symmetry of the Mn^{3+} lattice is either $P6_3cm$ or $P6_3\underline{cm}$ of which the latter corresponds to a ferromagnetic state which is ruled out by magnetization

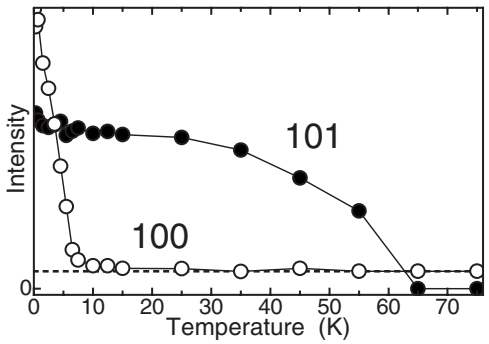

FIG. 2. Temperature dependence of the (101) and (100) reflections of h-$DyMnO_3$ measured in a cooling run on the sample from Fig. 1. The dashed line marks the offset due to crystallographic contributions.

measurements.[7,14,18] Table I further shows that zero (100) intensity is *consistent* with the $P6_3cm$ symmetry of the Dy^{3+} lattice proposed earlier[14] while it clearly *excludes* $P6_3cm$.

We thus conclude that three independent experimental parameters, i.e., SHG polarization, SHG spectrum, and neutron-diffraction intensity, lead to $P6_3cm$ as magnetic symmetry of the Mn^{3+} lattice in the high-temperature range of h-$DyMnO_3$. This is in striking contrast to the known (Ref. 14) and confirmed (Table I, Fig. 2) $P6_3cm$ symmetry of the Dy^{3+} lattice.

Although it is not unusual that magnetic order is parametrized by more than one representation it is most remarkable that this occurs in the h-$RMnO_3$ system. Tight coupling between the Mn^{3+} and R^{3+} lattices with "compatible" order of the 3*d* and 4*f* lattices, i.e., according to a single representation, was regarded as central mechanism in determining its magnetoelectric and multiferroic properties.[5–12] However, the "incompatibility" of magnetic representations observed here shows that the 3*d*-4*f* coupling must be distinctly less rigid than assumed.

The dilemma is solved by assuming the magnetic equivalent of a triggering mechanism observed in ferroelectrics.[22] The emergence of the antiferromagnetic Mn^{3+} order creates the basis for the emergence of the Dy^{3+} order. Yet, the latter and the former order occur independently, i.e., the Mn^{3+} order does not determine the representation, the orientation of the order parameter, or the domain structure of the Dy^{3+} order. According to Ref. 22 this is possible if the lowest-order coupling between the order parameters $\ell_{Mn,Dy}$ is *biquadratic* with a free-energy contribution $F=-(\gamma/2)\ell^2_{Mn}\ell^2_{Dy}$. Note that the triggering mechanism is a symmetry-based model, i.e., without insight into the *microscopy* of the Mn^{3+}-R^{3+} coupling and the variety of manifestations in the h-$RMnO_3$ series. However, the triggering mechanism provides *rigid boundaries* for such a model. It would have to be consistent with the absence of terms $\propto\ell_{Mn}\ell_{Dy}$, $\ell^2_{Mn}\ell_{Dy}$, and $\ell_{Mn}\ell^2_{Dy}$. Moreover, gradient terms[10] cannot dominate the microscopy because they would become large near the magnetic domain walls and the resulting inhomogeneity of the SHG signal was not observed.

Because of its general nature the magnetic triggering mechanism creates the framework for the magnetic h-$RMnO_3$ system in general. Aside from providing a higher-order 3*d*-4*f* coupling it leaves the explicit magnetic order open so that incompatible (e.g., R=Dy) as well as compatible [e.g., R=Yb and Ho (Refs. 6, 8, and 17)] sublattice order may occur. The ordering temperatures of the 3*d* and the 4*f* lattices may be identical (e.g., R=Dy) or not [e.g., R=Ho (Ref. 17)] and large-scale Mn-related domains may coexist with small scale *R*-related domains.[19]

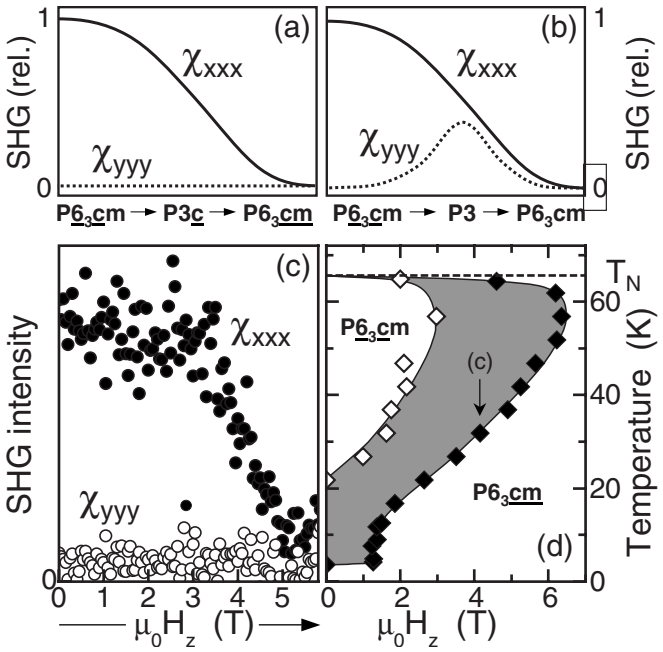

FIG. 3. Phase diagram of the magnetic Mn^{3+} order in h-$DyMnO_3$ in a magnetic field along *z*. [(a) and (b)] Sketch of the SHG contributions in the course of the spin reorientation toward the (a) $P6_3cm$ and (b) $P6_3cm$ phases. (c) Exemplary field dependence of the SHG signal at 32 K in a field-increasing run. (d) Phase diagram derived from data as in (c). Temperature-increasing and -decreasing runs yield the boundaries on the right- and left-hand side of the gray area, respectively. The boundary values correspond to observation of 50% of the SHG yield of the $P6_3cm$ phase.

Because of the biquadratic coupling a variety of phenomena that were related to a pronounced linear 3*d*-4*f* coupling have to be scrutinized. In addition, we cannot confirm that the Mn^{3+} order is related to the size of the R^{3+} ion.[6,23] If this were the case, the Mn^{3+} spins in $DyMnO_3$ with the largest R^{3+} ion of the h-$RMnO_3$ system would order according to the $P6_3cm$ structure already observed in $HoMnO_3$ and $YMnO_3$. Likewise, it can be excluded that the unusual magnetic phase diagram and magnetoelectric properties established for $HoMnO_3$ (Refs. 4, 16, and 24) continue toward rare-earth h-$RMnO_3$ compounds with a smaller R^{3+} radius than Ho^{3+}. These observations corroborate the relative independence of the Mn^{3+} and R^{3+} lattices.

In the low-temperature range and in a magnetic field applied along *z* the magnetic order of the Dy^{3+} spins changes from $P6_3cm$ to $P6_3cm$.[14,18] The emerging intensity of the (100) peak in Fig. 2 reflects the transition of the Dy^{3+} lattice to the $P6_3cm$ phase in accordance with magnetization measurements[14,18] and in agreement with Table I. This obscures the Mn^{3+}-related contributions so that we revert to SHG measurements for identifying the Mn^{3+} order.

Figures 1(d) and 3(c) show that the SHG intensity is quenched in the low-temperature range and in a magnetic field. According to Table I this indicates a transition to either the $P6_3\underline{cm}$ or the $P6_3cm$ phase. According to Figs. 3(a) and 3(b) the $P\underline{6_3}c\underline{m} \rightarrow P6_3\underline{cm}$ transition passes through a state with $P3\underline{c}$ symmetry for which $\chi_{xxx} \neq 0$, $\chi_{yyy}=0$ while the $P\underline{6_3}c\underline{m} \rightarrow P6_3cm$ transition passes through a state with $P3$ symmetry for which $\chi_{xxx} \neq 0$, $\chi_{yyy} \neq 0$.[15] Figure 3(c) reveals that the first scenario is realized. This is confirmed by the phase diagram in Fig. 3(d). Data points denote the magnetic field at which magnetic phase transitions are observed with the gray area marking the difference between field-increasing and -decreasing runs. Qualitatively, the same phase diagram was obtained on h-RMnO$_3$ with R=Er, Tm, and Yb all of which exhibit a $P\underline{6_3}c\underline{m} \rightarrow P6_3\underline{cm}$ transition of the Mn^{3+} lattice in a magnetic field whereas the phase diagram of h-HoMnO$_3$, in which this transition does not occur, is different. We conclude that in the low-temperature range and in a magnetic field along z the magnetic symmetry of the Mn^{3+} lattice in h-DyMnO$_3$ is $P6_3\underline{cm}$ and, thus, compatible to the magnetic symmetry of the Dy^{3+} lattice.

This compatibility is not a compulsory indication for an enhanced linear $3d$-$4f$ exchange. $P6_3\underline{cm}$ is a ferromagnetic point group and the observation that a magnetic field supports the transition into this state indicates that the magnetic field energy rather than additional Mn^{3+}-Dy^{3+} exchange coupling may be responsible for the $P6_3\underline{cm} \rightarrow P6_3\underline{cm}$ transition of the Mn^{3+} lattice. The field is generated internally by the ferromagnetic order of the Dy^{3+} lattice and supported externally by the applied magnetic field. Accordingly, the gray area in Fig. 3(d) does not show the hysteresis of the Mn^{3+} lattice but rather the response of the Mn^{3+} lattice to the magnetizing field exerted by the Dy^{3+} lattice when it is ferromagnetically ordered.

We thus observed that the magnetic order of the manganese and the rare-earth sublattices in the h-RMnO$_3$ system can be "incompatible." In h-DyMnO$_3$ Mn^{3+} ordering according to $P\underline{6_3}c\underline{m}$ and Dy^{3+} ordering according to $P\underline{6_3}c\underline{m}$ is revealed, yielding $P6_3$ as overall symmetry. The incompatibility demonstrates that the $3d$-$4f$ interaction in the h-RMnO$_3$ series is distinctly less rigid than assumed up to now. Instead, a yet unnoticed biquadratic magnetic triggering mechanism relates the R^{3+} to the Mn^{3+} order while, however, leaving the magnetic structures of the respective sublattices independent. The triggering mechanism constitutes boundaries for any microscopic mechanism explaining the Mn^{3+}-Dy^{3+} interplay. It provides a framework for the h-RMnO$_3$ system, in general, and various manifestations of the triggering mechanism are observed throughout the series. As a consequence, a variety of magnetoelectric coupling effects in the h-RMnO$_3$ system that were previously assigned to linear $3d$-$4f$ coupling have now to be scrutinized with respect to their origin.

We thank P. Tolédano for helpful advice about the triggering mechanism. Authors in Bonn thank the DFG SFB 608 for subsidy. D.N.A. thanks the DFG for financial support under Contract No. AR 613/1-1.

*fiebig@hiskp.uni-bonn.de

[1] M. Fiebig, J. Phys. D **38**, R123 (2005).
[2] S.-W. Cheong and M. Mostovoy, Nature Mater. **6**, 13 (2007).
[3] R. Palai, R. S. Katiyar, H. Schmid, P. Tissot, S. J. Clark, J. Robertson, S. A. T. Redfern, G. Catalan, and J. F. Scott, Phys. Rev. B **77**, 014110 (2008).
[4] F. Yen, C. R. dela Cruz, B. Lorenz, E. Galstyan, Y. Y. Sun, M. M. Gospodinov, and C. W. Chu, J. Mater. Res. **22**, 2163 (2007).
[5] Th. Lottermoser *et al.*, Nature (London) **430**, 541 (2004).
[6] X. Fabrèges, I. Mirebeau, P. Bonville, S. Petit, G. Lebras-Jasmin, A. Forget, G. André, and S. Pailhès, Phys. Rev. B **78**, 214422 (2008).
[7] S. Harikrishnan *et al.*, J. Phys.: Condens. Matter **21**, 096002 (2009).
[8] Th. Lonkai, D. Hohlwein, J. Ihringer, and W. Prandl, Appl. Phys. A: Mater. Sci. Process. **74**, s843 (2002).
[9] H. Sugie, N. Iwata, and K. Kohn, J. Phys. Soc. Jpn. **71**, 1558 (2002).
[10] I. Munawar and S. H. Curnoe, J. Phys.: Condens. Matter **18**, 9575 (2006).
[11] T. A. Tyson, T. Wu, K. H. Ahn, S.-B. Kim, and S.-W. Cheong, Phys. Rev. B **81**, 054101 (2010).
[12] S. Lee *et al.*, Nature (London) **451**, 805 (2008).
[13] X. Fabrèges, S. Petit, I. Mirebeau, S. Pailhès, L. Pinsard, A. Forget, M. T. Fernandez-Diaz, and F. Porcher, Phys. Rev. Lett. **103**, 067204 (2009).
[14] S. Nandi *et al.*, Phys. Rev. B **78**, 075118 (2008).
[15] R. R. Birss, *Symmetry and Magnetism* (North-Holland, Amsterdam, 1966).
[16] M. Fiebig, Th. Lottermoser, and R. V. Pisarev, J. Appl. Phys. **93**, 8194 (2003).
[17] S. Nandi, A. Kreyssig, L. Tan, J. W. Kim, J. Q. Yan, J. C. Lang, D. Haskel, R. J. McQueeney, and A. I. Goldman, Phys. Rev. Lett. **100**, 217201 (2008).
[18] V. Yu. Ivanov, A. A. Mukhin, A. S. Prokhorov, A. M. Balbashov, and L. D. Iskhakova, Phys. Solid State **48**, 1726 (2006).
[19] M. Fiebig, V. V. Pavlov, and R. V. Pisarev, J. Opt. Soc. Am. B **22**, 96 (2005).
[20] B. Hillebrands, J. Phys. D: Appl. Phys. **41**, 160301 (2008).
[21] T. Iizuka-Sakano, E. Hanamura, and Y. Tanabe, J. Phys.: Condens. Matter **13**, 3031 (2001).
[22] J. Holakowský, Phys. Status Solidi B **56**, 615 (1973).
[23] D. P. Kozlenko, S. E. Kichanov, S. Lee, J. G. Park, and B. N. Savenko, J. Phys.: Condens. Matter **19**, 156228 (2007).
[24] O. P. Vajk, M. Kenzelmann, J. W. Lynn, S. B. Kim, and S.-W. Cheong, Phys. Rev. Lett. **94**, 087601 (2005).